Available online at www.sciencedirect.com

SCIENCE DIRECT®

Journal of Catalysis 224 (2004) 18–27

JOURNAL OF CATALYSIS

www.elsevier.com/locate/jcat

Influence of reductant on the thermal stability of stored NOx in Pt/Ba/Al_2O_3 NOx storage and reduction traps

Zhaoqiong Liu and James A. Anderson *

Surface Chemistry and Catalysis Group, Division of Physical and Inorganic Chemistry, University of Dundee, DD1 4HN, Scotland, UK

Received 3 October 2003; revised 7 January 2004; accepted 7 January 2004

Abstract

The stability and reactivity of NOx stored over Pt/Ba/Al_2O_3 storage and reduction catalysts have been compared in the presence of hydrogen, carbon monoxide, and propene as reductants under stoichiometric conditions while heating between 298 and 873 K. The order of efficiency in terms of conversion of stored NOx to N_2 was $H_2 > CO >$ propene. Additionally the use of hydrogen led to the lowest NO_2:NO ratio. Four potential mechanisms to explain the initial release of stored NOx are discussed. In the absence of reductant, less than 10% of released NOx was in the form of NO, whereas the presence of reductant led to significant NO release which was independent of the presence of Pt. Results suggest that while formation of N_2 from stored NOx requires the presence of reduced noble metal sites, formation of NO can take place over the support alone, probably by direct interaction between reductant and stored nitrate. The role of Pt in providing activated spill over reductant is important for the decomposition of certain forms of NOx stored by the alumina. Both hydrogen and propene oxidation were inhibited by the presence of NOx whereas CO was able to compete for Pt sites, even in the presence of high NOx concentrations.

1. Introduction

NOx storage and reduction catalysts offer one method of controlling emissions from automobile sources while permitting operation under predominantly lean-burn conditions [1–5]. NOx is stored under lean conditions on an alkaline earth oxide component such as baria and then released during intermittent rich/stoichiometric periods where the NOx is released and converted to nitrogen by the presence of a reductant gas in the presence of a noble metal catalyst [2,3]. Although oscillating lean/rich (or stoichiometric) conditions are employed during normal driving, the engine is operated under constant air/fuel ratio (fixed λ) conditions during the warm-up period. This use of λ fixed at stoichiometry during warm-up allows the engine to attain light-off conditions as rapidly as possible before switching to lean conditions at a temperature where NOx storage becomes effective. Few studies [6–9] have considered stored NOx stability under warm-up conditions, although in a recent study [7], the stability of stored NOx under warm up at different fixed λ values was considered where propene was used as reductant. The influence of different reductants on NOx release has received limited attention [9], although stored NOx stability in the presence of propene has been more widely studied [6–9] even though CO is expected to be the dominant reductant under rich purge. The present study directly compares stored NOx stability in the presence of H_2, CO, or propene in an attempt to determine what triggers the initial release of NOx gases from the stored NOx. NO_2 rather than NO was used in order to saturate the NOx storage component in each experiment in a reproducible manner and also to avoid the need for a catalysed NO to NO_2 stage which thus allowed a more direct comparison between the behaviour of Pt-containing and Pt-free samples.

2. Experimental

BaO/Al_2O_3 samples (10 wt% BaO) were prepared by precipitation of $Ba(OH)_2$ from a nitrate solution onto Degussa Aluminoxid C γ-alumina using an ammonia solution. The material was filtered, washed, dried at 363 K (16 h), and calcined in air (100 $cm^3\ min^{-1}$) at 773 K (2 h). A portion of sample was wet impregnated with 1 wt% Pt (H_2PtCl_6) and excess water removed by heating while continually stirring. The resulting powder was dried overnight at 363 K and cal-

---

[*] Corresponding author.
E-mail address: j.a.anderson@dundee.ac.uk (J.A. Anderson).

0021-9517/$ – see front matter © 2004 Elsevier Inc. All rights reserved.
doi:10.1016/j.jcat.2004.01.020

cined in air (100 $cm^3\,min^{-1}$) at 773 K (2 h). Pt dispersion was measured using CO pulsed chemisorption on samples reduced in H_2 at 673 K. DRIFT spectra (4 cm^{-1} resolution, 40 scans) were recorded using an MCT detector and a Harrick environmental cell. A pc-controlled gas blender fed the required inlet gases, with exit gas analysis performed using a combination of on-line chemiluminescence detector, which was used exclusively for NO and NO_2 concentration determination, and a quadropole mass spectrometer. Samples were calcined in situ in a flow of dry air (50 $cm^3\,min^{-1}$) in the DRIFT cell at 673 K (1 h) and exposed to NO_2 (750 ppm) at 673 K for 15 min. The cell was then cooled at 10 K min^{-1} to 298 K in NO_2 (750 ppm) before flushing in air to remove gaseous and weakly adsorbed forms of NOx before a TPD was performed between 298 and 873 K at 4 K min^{-1} under air/N_2 flows (50 $cm^3\,min^{-1}$) containing either H_2, CO, or propene. Gas mixtures contained 3.35% of H_2 (or CO)/ 7.98% air/balance N_2 or 7.10% of 5% propene in N_2/7.98% air/balance N_2.

3. Results

3.1. Sample characteristics

The X-ray diffraction pattern of the parent Ba/Al_2O_3, exhibited (2θ) peaks at 24.1, 34.7, and 42.1° due to $BaCO_3$ and at 19.4, 22.0, and 28.0° due to $BaAl_2O_4$ [5,6]. The BET area of the calcined Ba/Al_2O_3 was 129 $m^2\,g^{-1}$ with an average pore diameter of 39 nm compared to 141 $m^2\,g^{-1}$ and 30 nm for the parent alumina. After Pt salt impregnation and calcination, there was a change to the baria dispersion as only diffraction peaks due to the alumina support were determined for the catalysts. This has been attributed [7] to redispersion of the baria following the addition of acidic Pt precursor. In addition to the influence of retained chloride on adsorption on the exposed baria component [7], the potential modification to the properties of the active Pt component must not be neglected. The Pt dispersion (assuming CO:Pt = 1:1) was 64.9% for a sample reduced at 673 K.

3.2. Combined TPD/FTIR experiments

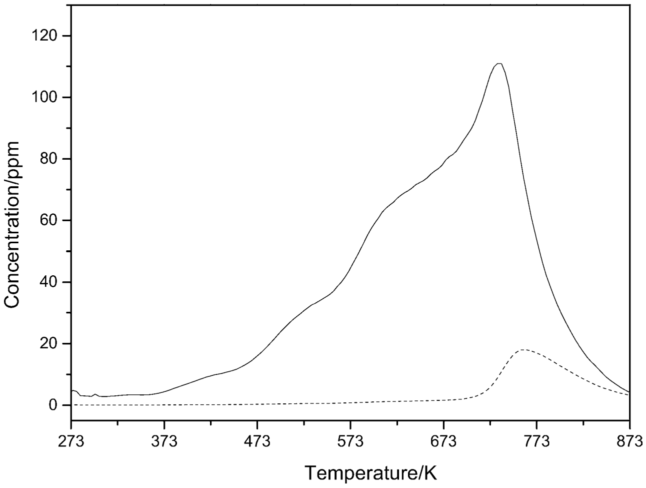

Fig. 1. TPD of NO (dashed line) and NO_2 (solid line) released from Pt/ Ba/Al_2O_3 after exposure to 750 ppm NO_2 in N_2/air at 673 K, cooled to 298 K and then heated to 873 K at 4 K min^{-1} in a 7.98% air/balance N_2 gas mixture (50 $cm^3\,min^{-1}$).

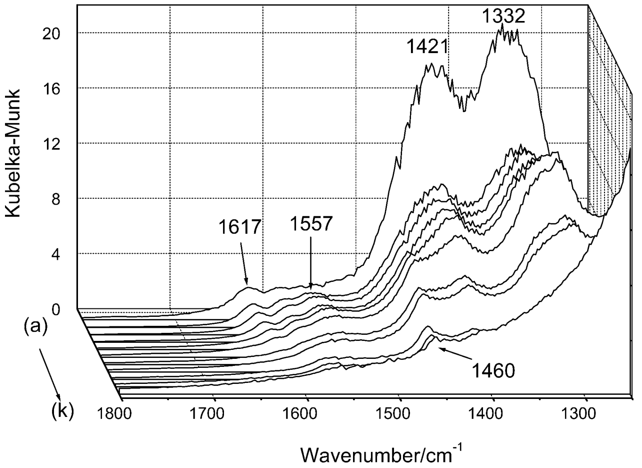

Fig. 2. FTIR spectra of Pt/Ba/Al_2O_3 after exposure to 750 ppm NO_2 in N_2/ air at 673 K and cooled to 298 K. Sample was heated in a stoichiometric H_2/ air/N_2 mixture (50 $cm^3\,min^{-1}$) to 873 K with spectra recorded at (a) 298, (b) 373, (c) 423, (d) 453, (e) 513, (f) 543, (g) 593, (h) 623, (i) 653, (j) 723, and (k) 803 K.

Fig. 1 shows the TPD of stored NOx in the presence of 1.596% oxygen/balance N_2. NO_2 formed the majority of the released NOx gas and was released across the temperature range 373 to 873 K which could be deconvoluted into component maxima at 427, 525, 650, and 744 K. NO was released in a single peak at 760 K and formed less than 7% of the total NOx released. The total NOx stored was 0.714 mmol g^{-1} (Table 1) in good agreement [7] with a previous value of 0.700 mmol g^{-1} for an experiment conducted under air (21% oxygen). Apart from differences in the extent to which the peaks were resolved, the NOx desorption profiles under the higher oxygen concentration were somewhat similar with maxima at 530 and 752 K for NO_2 and 785 K for NO [7].

Fig. 2, a, shows the IR spectrum of the sample exposure to NO_2 at 673 K followed by cooling to 298 K, purging in nitrogen, and then exposing to a stoichiometric H_2/air/N_2 mixture. The absence of weak bands between 1900 and 1650 cm^{-1} confirmed that weakly bound and gas-phase NO_2 were removed by the purge treatment. Bands at 1617, 1585, and 1557 cm^{-1} compare with a triplet at 1619, 1585, and 1568 cm^{-1} observed using a previous batch of a similar Pt/Ba/Al_2O_3 and assigned [7] to vibrations of adsorbed nitrate on the alumina surface. The spectrum was dominated by the bands at 1421/1332 cm^{-1} which compares with a doublet at 1434/1359 cm^{-1} in our previous study [7] and can be assigned to vibrations of monodentate nitrates on baria.

Table 1
NOx released from $Pt/BaO/Al_2O_3$ during TPD experiments under different gaseous environments

Fig.	Reductant	Peaks		Total	Peaks		Total	Total
No.		T (K)	NO_2[a]	NO_2[b]	T (K)	NO[a]	NO[b]	NOx[b]
1	Absent	525	0.337					
		650	0.266	0.666				0.714
		744	0.063		760	0.048	0.048	
3	H_2	357	0.0160		361	0.0190		
		400	0.0043	0.044	400	0.0070	0.143	0.187
		473	0.0013		473	0.0068		
					600	0.0880		
6	CO	533	0.18	0.182	553	0.154	0.154	0.336
9	C_3H_6	505	0.225	0.225	505	0.022		
					560	0.123	0.337	0.562
					650	0.156		
11	CO to H_2[c]	497	0.037	0.152	497	0.076	0.194	0.346
					600	0.044		
12	H_2 to CO[c]	373	0.039	0.113	373	0.044	0.183	0.296
		545	0.066		545	0.134		

[a] NOx released (mmol g_{cat}^{-1}) from integrated peak area at the defined temperature.
[b] NOx released (mmol g_{cat}^{-1}) from total integration over the range 298–873 K.
[c] Reductant gas was switched at 473 K.

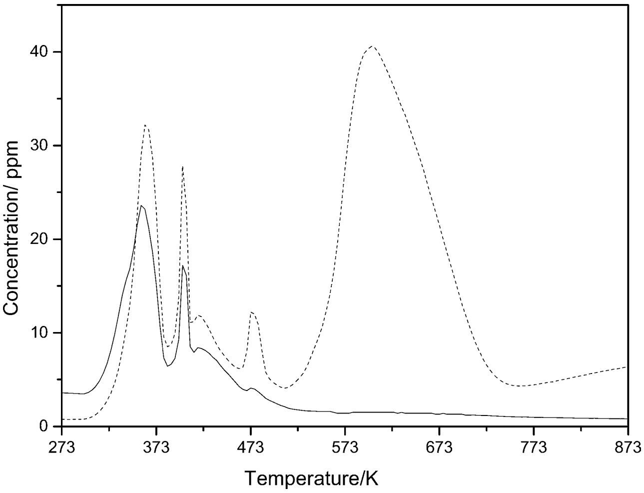

Fig. 3. TPD of NO (dashed line) and NO_2 (solid line) released from $Pt/Ba/Al_2O_3$ after exposure to 750 ppm NO_2 in N_2/air at 673 K, cooled to 298 K, and then heated to 873 K at 4 K min^{-1} in a stoichiometric H_2/air/N_2 mixture (50 cm^3 min^{-1}).

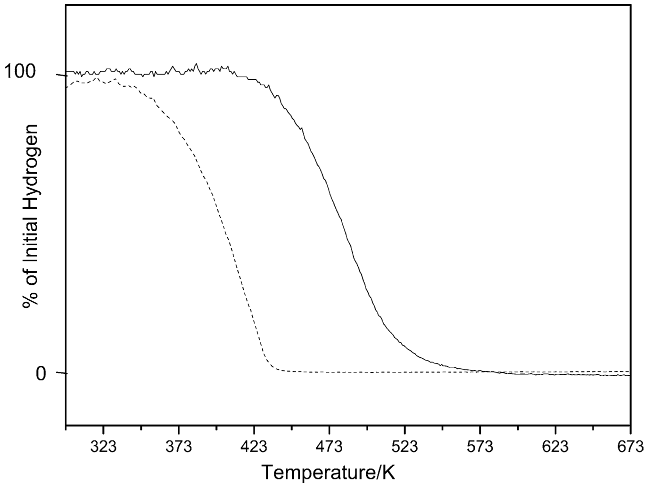

Fig. 4. H_2 conversion while heating at 4 K min^{-1} under stoichiometric conditions for $Pt/Ba/Al_2O_3$ which had been calcined only (dashed line) or calcined and exposed to 750 ppm NO_2 in N_2/air at 673 K and cooled to 298 K (solid line).

This species diminished significantly by heating to 373 K in H_2/air/N_2, and was accompanied by the simultaneous release of both NO and NO_2 into the gas phase (Fig. 3). The ratio of NO:NO_2 released in the first decomposition peak (360 K) was 1.18:1 (Table 1). No significant loss of band intensity was observed in spectra recorded over the temperature range 373–543 K (Fig. 2, b–f) despite the fact that the TPD (Fig. 3) showed evidence for NOx release at 400, 418, and 475 K, each release containing both NO and NO_2 but with a decreasing NO_2:NO ratio. This temperature range also coincided with a corresponding conversion of hydrogen from ca. 0 to 100% (Fig. 4), total conversion being achieved prior to the final desorption peak of NO (Fig. 3). The latter was released over the range 509–742 K with a maximum rate at 600 K (Fig. 3). Infrared spectra indicated lost intensity of the 1421/1332 cm^{-1} doublet between 543 and 593, and 623 and 653 K which may have been responsible for the release of NO. However, bands due to nitrate on the alumina were also of reduced intensity in spectra recorded above 543 K, indicating that desorption of this species may also have contributed to the observed NO signal. In any case, complete conversion of the reductant below the temperature of the final NO desorption peak indicates that the species selectively decomposed to NO rather than NO_2 followed by

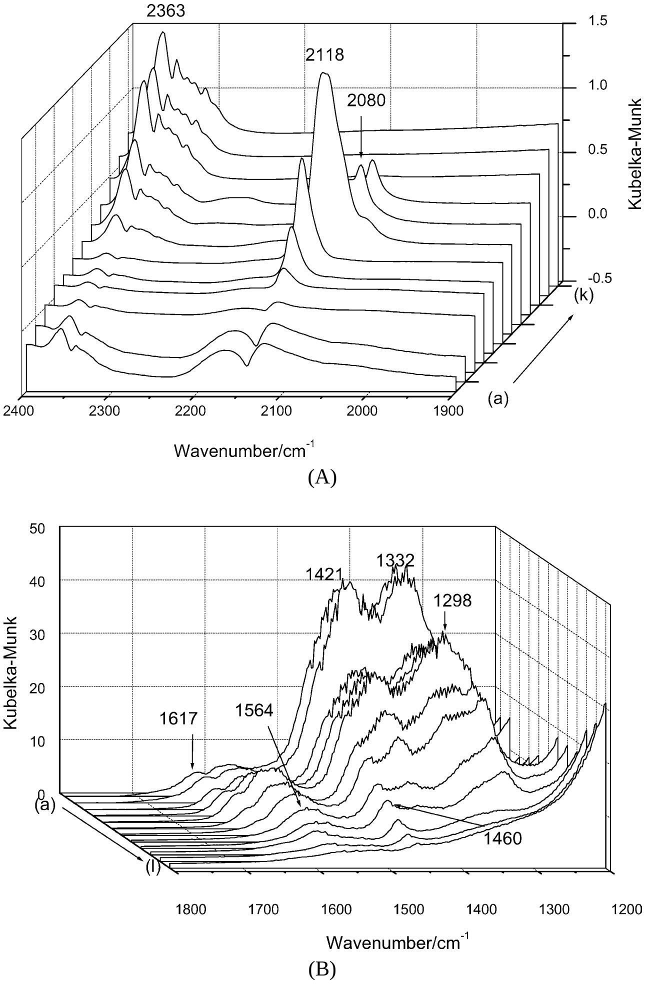

Fig. 5. (A and B) FTIR spectra of Pt/Ba/Al_2O_3 after exposure to 750 ppm NO_2 in N_2/air at 673 K and cooled to 298 K. Sample then heated at 4 K min^{-1} in stoichiometric CO/air/N_2 mixture (50 cm^3 min^{-1}) to 873 K with spectra recorded at (a) 298, (b) 316, (c) 373, (d) 410, (e) 447, (f) 496, (g) 557, (h) 590, (i) 617, (j) 703, (k) 793, and (l) 838 K.

catalytic reduction to NO. Note that heating in air in the absence of reductant would release NO_2 over this temperature range [7]. The presence of NOx in the system retarded the H_2 oxidation light off by ca. 70 K (Fig. 4). Above 543 K, reduced band intensity due to adsorbed NOx allowed a band at 1460 cm^{-1} to be revealed due to the presence of residual carbonate. This feature was also clearly identified in NOx storage studies over alumina alone [7] and the absence of any accompanying vibrational feature would allow assignment to the asymmetric stretching mode of a simple, symmetrical carbonate structure interacting with the exposed alumina support.

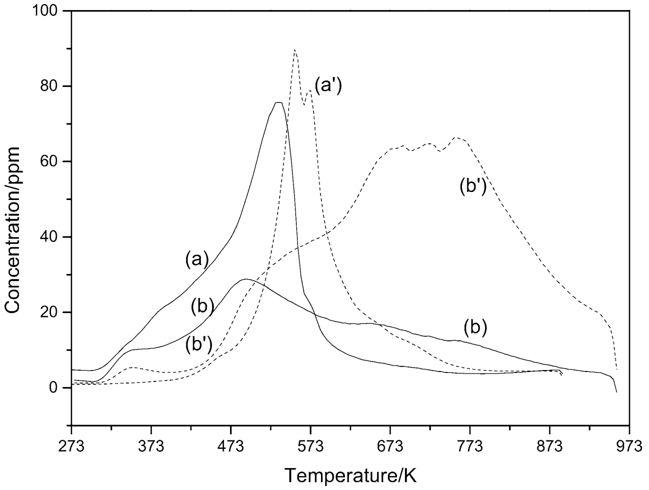

Fig. 6. TPD of NO (a′, b′, dashed lines) and NO_2 (a, b, solid lines) released from (a) Pt/Ba/Al_2O_3 and (b) Ba/Al_2O_3 after exposure to 750 ppm NO_2 in N_2/air at 673 K, cooled to 298 K and then heated to 873 K at 4 K min^{-1} in a stoichiometric CO/air/N_2 mixture (50 cm^3 min^{-1}).

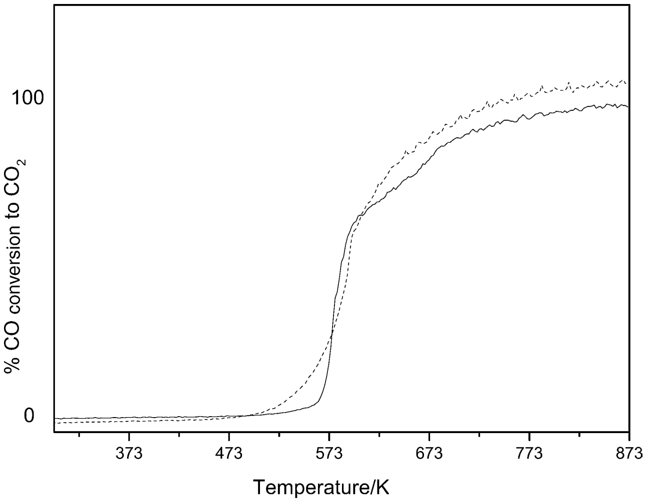

Fig. 7. Percentage CO conversion to CO_2 while heating at 4 K min^{-1} under stoichiometric conditions for Pt/Ba/Al_2O_3 which had been calcined only (dashed line) or calcined and exposed to 750 ppm NO_2 in N_2/air at 673 K and cooled to 298 K (solid line).

Similar infrared spectra to those just described were observed when the same sample pretreated in NO_2 was exposed to a gas containing a stoichiometric mixture of CO and oxygen (Fig. 5B). Again, band loss at 1421/1332 cm^{-1} between 316 and 373 K coincided with NOx release, although on this occasion, the released gas was predominantly NO_2 in this temperature range (Fig. 6). The majority of NOx was released between 423 and 673 K (Fig. 6) in a NO_2:NO ratio of 1.2:1 (Table 1). In the absence of Pt, NO_2 was released over the full 300–873 K range with a maximum at 494 K. NO formed by far the greater proportion of the released gas with the majority released between 500 and 800 K. The presence of CO in the gas phase allowed information regarding the Pt surface to be obtained (Fig. 5A). Initially, the amount of exposed, oxidized sites was low as revealed [10] by the low intensity at the 2118 cm^{-1} band (Fig. 5A, c). However, as a function of temperature, this grew, reaching a maximum in spectra recorded at 557 K (Fig. 5A, g). This increased intensity was not accompanied by a detectable release of CO_2 as revealed by the absence of an appreciable mass 44 signal in the mass spectrometer trace (Fig. 7), and by the constant intensity at 2363 cm^{-1} in the DRIFT spectra (Fig. 5 A). At

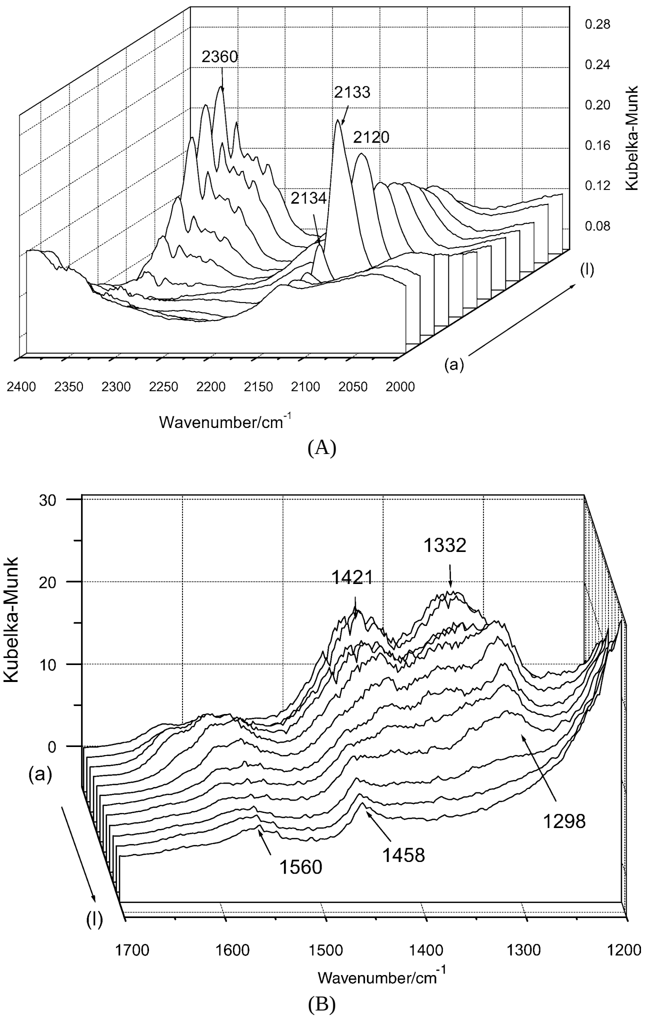

Fig. 8. (A and B) FTIR spectra of Pt/Ba/Al_2O_3 after exposure to 750 ppm NO_2 in N_2/air at 673 K and cooled to 298 K. Sample was then heated at 4 K min^{-1} in a stoichiometric C_3H_6/air/N_2 mixture (50 cm^3 min^{-1}) to 873 K with spectra recorded at (a) 298, (b) 323, (c) 388, (d) 433, (e) 523, (f) 573, (g) 598, (h) 623, (i) 673, (j) 698, (k) 723, (l) 773, and (m) 873 K.

the temperature where the 2118 cm^{-1} band reached a maximum (557 K), a shoulder was detected at 2071 cm^{-1} due to CO on exposed Pt (0) sites (Fig. 5A, g), and the band due to gaseous CO_2 (2363 cm^{-1}) was increased. The production of CO_2 was confirmed by the increased $m/e = 44$ in the ms trace (Fig. 7). The band at 2118 cm^{-1} was diminished, but not depleted with the sample between 590 and 617 K (Fig. 5A, h and i), although the band due to CO at reduced Pt sites (2083 cm^{-1}) became the dominant feature. At the higher of the temperatures, a doublet at 2230/2249 cm^{-1} was also detected, probably due to the formation of NCO located on the alumina support [11]. The majority of NOx had been given off into the gas phase by this temperature as indicated by the tailing of the NOx traces (Fig. 6). Above 617 K, bands due to NCO and CO on Pt sites were no longer detected, although the CO oxidation reaction continued as indicated by the continued growth of the band at 2363 cm^{-1} (Fig. 5A, j–l) and the increased $m/e = 44$ signal (Fig. 7).

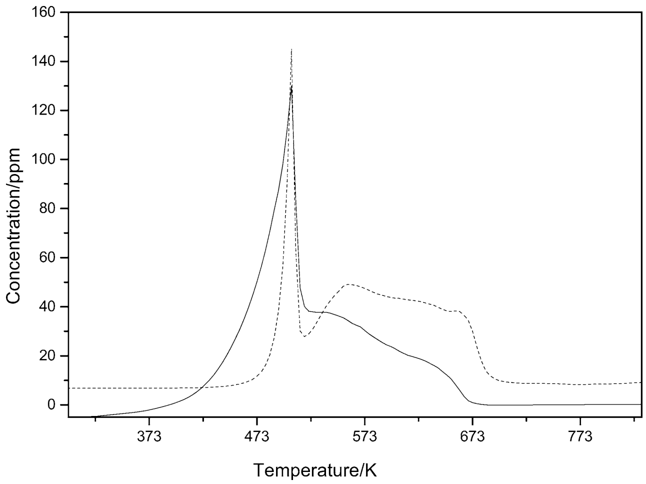

Fig. 9. TPD of NO (dashed line) and NO_2 (solid line) released from Pt/Ba/Al_2O_3 after exposure to 750 ppm NO_2 in N_2/air at 673 K, cooled to 298 K, and then heated to 873 K at 4 K min^{-1} in a stoichiometric propene/air/N_2 mixture (50 cm^3 min^{-1}).

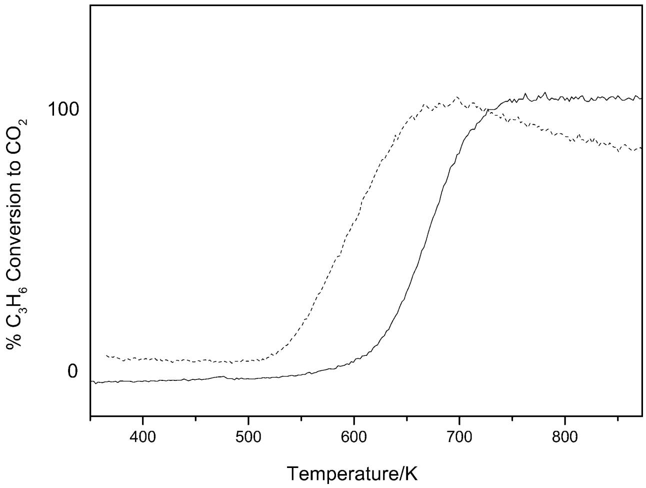

Fig. 10. Propene conversion (%) to CO_2 while heating at 4 K min^{-1} under stoichiometric conditions for Pt/Ba/Al_2O_3 which had been calcined only (dashed line) or calcined and exposed to 750 ppm NO_2 in N_2/air at 673 K and cooled to 298 K (solid line).

Bands at 1617, 1585, and 1557 cm^{-1} and at 1421/1332 cm^{-1} were present for a sample pretreated in NO_2 but prior to exposure to a stoichiometric gas stream containing propene as reductant (Fig. 8B). As in the presence of the gas mixtures described above, all of these features were diminished in intensity on heating to leave features at 1557 and 1458 cm^{-1}. A feature at 1298 cm^{-1} was revealed in the range 523–673 K as a consequence of reduced intensity at 1332 cm^{-1} (Fig. 8B, e–i), but this feature was removed on heating between 673 and 698 K (Fig. 8B, i and j). This temperature range coincided with the maximum desorption temperature for stored NOx (Fig. 9). Below this temperature, both NO and NO_2 had been released in sharp maxima at 505 K, followed by less intense maxima between 523 and 673 K. The combustion of propene to give CO_2 was initiated around 600 K as observed in both the FTIR spectra (band at 2362 cm^{-1}) (Fig. 8A, f and g) and the $m/e = 44$ signal in the mass spectrometer (Fig. 10). The latter plot (Fig. 10) emphasized the delayed propene light off by ca. 85 K in the presence of stored NOx, although following light off both NO and NO_2 were still being released into the gas phase (Fig. 9). Although the production of CO_2 was detected by mass spectrometer only above ca. 600 K, FTIR spectra revealed that partial oxidation of propene had begun by 433 K as revealed by the band at 2134 cm^{-1} (Fig. 8A, d). The latter feature reached maximum intensity in spectra recorded with the sample at 573 K (Fig. 8A, e) before being gradually diminished and progressively blue-shifted to leave a band at 2120 cm^{-1} in spectra of the sample at 673 K (Fig. 8A, i). Unlike the sample where CO was used as reductant (Fig. 5A), the loss of this feature was not accompanied by the development of a band which could be attributed to CO adsorbed on metallic Pt sites.

To determine whether differences in NOx stability in the presence of the different reductant molecules were the result of differences in the ability of the different molecules to produce reduced Pt surface, experiments were performed where a switch in the reductant stream was performed. Switches were performed in separate experiments at 400 and 473 K; however, for the sake of brevity, only the latter are shown in Figs. 11 and 12. When a NOx-saturated surface was exposed to a CO-containing stream, there was only a slow, release of NO_2 below 473 K (Fig. 11) as observed in the TPD trace performed in a CO-containing stream between 298 and 873 K (Fig. 6). When the CO was replaced by H_2 in the stream at 473 K, a sharp release of both NO and NO_2 was observed around 490 K. When the CO was replaced by H_2 at 400 K, the NOx was released with a similar NO:NO_2 ratio at 415 K. The amount of NOx released in a single pulse at 490 K was 0.113 compared to 0.099 $mmol\,g^{-1}$ between 298 and 473 K when the sample was exposed to hydrogen at 298 K and then heated in the hydrogen-containing stream (Fig. 3). Relatively little NOx was released above 490 K.

An experiment was performed in which hydrogen in a stoichiometric gas stream was exchanged at 473 K for CO over a NOx-saturated catalyst. The NOx desorption profile below 473 K (Fig. 12) resembled that obtained over a similar temperature range by heating in H_2 from 298 to 873 K (Fig. 3) with maxima at 360, 400, and 420 K. However, on changing to CO, a sharp release of NO (484 K) was observed which was followed by the simultaneous release of both NO_2 (535) and NO (544/562). The profile shape of the NO released (Fig. 12) was similar to that obtained by heating in a CO-containing gas stream over the whole temperature range (Fig. 6). The tail end of the NO_2 peak (Fig. 12) was also similar to that obtained by heating in a CO-containing gas stream over the whole temperature region (Fig. 6), but the leading edge which stretched from 298 to 473 K was absent.

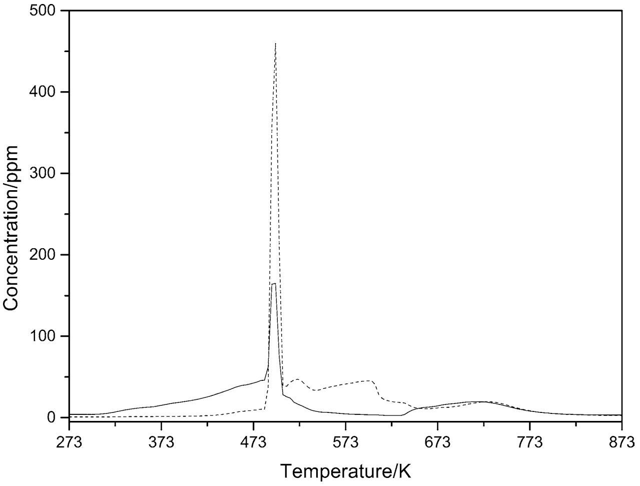

Fig. 11. TPD of NO (dashed line) and NO_2 (solid line) released from Pt/Ba/Al_2O_3 after exposure to 750 ppm NO_2 in N_2/air at 673 K, cooled to 298 K, and then heated at 4 $K\,min^{-1}$ in a stoichiometric CO/air/N_2 mixture (50 $cm^3\,min^{-1}$) to 473 K and changed to stoichiometric H_2/air/N_2 mixture (50 $cm^3\,min^{-1}$) and heated to 873 K.

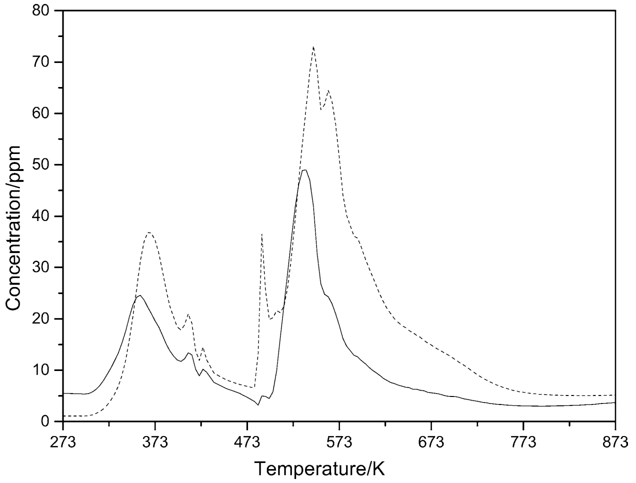

Fig. 12. TPD of NO (dashed line) and NO_2 (solid line) released from Pt/Ba/Al_2O_3 after exposure to 750 ppm NO_2 in N_2/air at 673 K, cooled to 298 K, and then heated at 4 $K\,min^{-1}$ in a stoichiometric H_2/air/N_2 mixture (50 $cm^3\,min^{-1}$) to 473 K and changed to a CO/air/N_2 stoichiometric mixture (50 $cm^3\,min^{-1}$) and heated to 873 K.

4. Discussion

Integration of the TPD profiles in the absence of reductant, where no conversion to nitrogen can occur, is indicative of the NOx storage capacities of the Pt/Ba/Al_2O_3 sample. The obtained value of 0.714 $mmol\,g^{-1}$ (Table 1) is in good agreement with our previously reported value of 0.700 $mmol\,g^{-1}$ [7] for a different batch of similarly prepared catalysts containing 10% BaO. Lower values, but using different experimental conditions, have been reported by others [12,13] for 1% Pt/20% BaO/Al_2O_3 samples. However, as formation of bulk barium nitrate is not expected under our conditions [5,8,14], baria dispersion is probably a key factor in determining maximum storage capacity

[8,13–15], and therefore a correlation between loading and capacity is not expected.

In the absence of reductant, by far the majority of NOx (ca. 93%) was released as NO_2 (Fig. 1) in agreement with previous experimental [7,13,14] and modeling [13] studies. The profile was almost identical when the experiment was performed in the absence of oxygen, indicating that NO is produced directly by thermal decomposition alone. Cant and Patterson [9] have suggested that NO release around 773 K is the consequence of Ba/Al_2O_3 catalysed decomposition of NO_2. The release of NO at temperatures below ca. 723 K in the presence of reductant must be a consequence of reduction processes either pre or post desorption.

As shown previously by our group [6–8] and others [3,9,14], the presence of reductant molecules in the gas stream destabilised the stored NOx, lowering the desorption temperatures and changing the relative proportions of $NO:NO_2$ released into the gas phase. The percentage reduction to nitrogen could be obtained from the difference between released NOx in the absence and presence of reductant (Table 1) as no N_2O was detected by IR here and was detected only in trace amounts in other laboratories [12,14]. Values obtained were 73% for H_2, 53% for CO, and 21% for propene. The poor conversion using propene as reductant has already been observed [7]. In addition to releasing the lowest amount of the stored NOx as nitrogen oxides, the use of hydrogen led to the lowest $NO_2:NO$ ratio.

Four possible mechanisms are worthy of consideration when discussing the release and reduction of stored NOx:

(A) The first route involves the destabilization of NOx stored in the form of nitrate as a consequence of the reduction in oxygen levels when gas-phase oxygen is consumed in the reaction with the reductant over available Pt sites. This would then drive the following reaction from left to right with the release of NOx gases.

$$(NO_3{}^-)_2 \Leftrightarrow O^{2-} + \tfrac{1}{2}O_2 + 2NO_2, \tag{1}$$

or

$$(NO_3{}^-)_2 \Leftrightarrow O^{2-} + O_2 + NO_2 + NO. \tag{2}$$

Although this path has been accepted by some [16], we have previously rejected this pathway as playing a major role under these conditions [7,17] on the basis that the light off temperature for propene oxidation is around 673 K (Fig. 10) and there is little evidence for propene consumption below this temperature where the majority, if not all NOx (Fig. 9), is released.

(B) The formation of product by reaction between gas-phase oxygen and reductant leads to the conversion of barium nitrate to barium hydroxide or barium carbonate, thus releasing NOx into the gas phase. As above, this pathway is not believed to be the main pathway to NOx release as the formation of CO_2 from propene oxidation occurred around 673 K (Fig. 10) and that the majority, if not all NOx (Fig. 9), is released below this temperature.

(C) NOx stored as nitrate is in equilibrium with trace amounts of NO_2 which is spilled over onto available Pt sites (law of microreversibility). The reductant reduces [3,12,18] this adsorbed NO_2 to release NO and/or N_2 which thus drives the decomposition of the nitrate. Incomplete reduction of Pt may lead to NO rather than N_2 being released [12].

$$(NO_3{}^-)_2 \Leftrightarrow O^{2-} + \tfrac{1}{2}O_2 + 2NO_2(\text{ads}) \rightarrow NO/N_2. \tag{3}$$

Higher light-off temperatures, especially for H_2 (Fig. 4) and propene (Fig. 10) in the presence of stored NOx, are consistent [7,17] with the inhibiting affect of adsorbed NOx at Pt sites, implying reverse spillover of NOx [18]. However, similarities in the desorption temperatures under air of NOx stored on Ba/Al_2O_3 in the absence and presence of Pt [7] would suggest that the removal of reversibly spilled over NOx from Pt sites does not drive the decomposition of the stored NOx.

(D) The final mechanism would be that the reductant molecule (or activated reductant molecule spilled over from Pt [18]) interacts directly with NOx stored on the baria component where nitrate is reduced to nitrite by removal of oxygen. The nitrite species then releases NO and gaseous oxygen as follows.

$$(NO_3{}^-)_2 \rightarrow (NO_2{}^-)_2 \rightarrow O^{2-} + \tfrac{1}{2}O_2 + 2NO. \tag{4}$$

With H_2 as reductant, stored NOx was released in five well-defined peaks (Fig. 3). In the range 300–420 K where no detectable H_2 consumption took place (Fig. 4) NOx desorption peaks at 360 and 400 K were observed (Fig. 3) where NO_2 and NO appear simultaneously in a mole ratio of approximately 1:1. This is consistent with the scheme: $(NO_3{}^-)_2 \Leftrightarrow O^{2-} + O_2 + NO_2 + NO$, [Eq. (2)], although as reduction in oxygen levels due to reaction with hydrogen had not commenced (Fig. 4), it is unlikely that mechanism A can be invoked. In the temperature range 423–523 K, hydrogen conversion from ca. 0–100% occurred (Fig. 4) and NOx was released in two well-defined temperature windows giving maxima at 418 and 475 K. While hydrogen was being consumed, simultaneous release of both NO_2 and NO occurred, although the balance was shifted now with NO being the predominant NOx gas. As no single reaction can be written to account for release of NO and NO_2 other than in a 1:1 ratio, it must be assumed that reactions as shown by both Eqs. (2) and (4) are taking place, the latter inferring that during conversion of hydrogen, some of the stored nitrate was reduced to nitrite. Note that an alternative to account for formation of both NO and NO_2 in nonequimolar quantities would be reaction scheme (3); however as both gases were detected simultaneously rather than with NO showing a slight time lag (as observed when CO was used as reductant—see Fig. 6), the possibility of a consecutive type-reaction to give both products is ruled out. Finally, between 523 and 740 K, conditions during which all gas-phase hydrogen was consumed (Fig. 4), NOx was released with NO being the only oxide of nitrogen detected. This would suggest that the balance between reaction schemes (2) and (4) was shifted to favor the

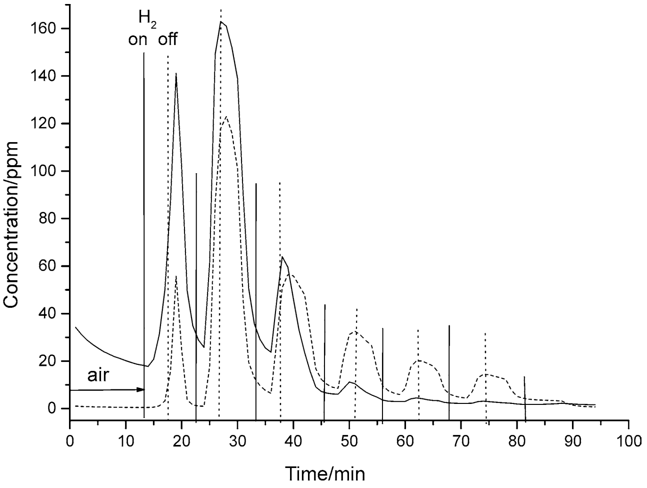

Fig. 13. NO (dashed line) and NO_2 (solid line) released from $Pt/Ba/Al_2O_3$ after exposure to 750 ppm NO_2 in N_2/air at 673 K, cooled to 298 K, and then heated at 4 K min^{-1} in air to 610 K. Then consecutive 5 min H_2/air/N_2 and air/N_2 pulses at 610 K solid and dotted vertical lines indicate switching on and off of hydrogen containing pulses, respectively.

latter and that NO was released by thermal decomposition of nitrite species formed by reduction of nitrate.

The possibility that ammonia formed at lower temperatures and trapped on the catalyst surface was released over this temperature range and acted as reducing agent for the remaining stored NOx is discounted, as by other workers [14], due to the lack of IR evidence for adsorbed NH_3 and the ms signals at 18 and 17 were constant at a 3:1 ratio as expected for H_2O with the sample above 450 K.

When an experiment was performed in which a NOx presaturated catalyst was heated to 610 K in air (releasing only NO_2) and then the temperature held at 610 K and exposed to alternating pulses of H_2/air/N_2 and air/N_2, the first pulse contained predominantly NO_2 (Fig. 13), whereas the TPRS experiment with hydrogen present from 298 K (Fig. 2) had shown that only NO was released at this temperature, suggesting that NO release was the consequence of sequential reaction rather than one direct step. Subsequent H_2/air pulses showed diminishing amounts of NOx but each time with a greater NO:NO_2 ratio until only NO was released. Should the reduction of Pt in hydrogen occur below 610 K leading to release of NO (and N_2) rather than NO_2 then one would imagine that Pt should reduce as soon as the first or second pulses were added rather than a progressive change in NO/NO_2 ratio (implying gradual Pt reduction) over a 35 min isothermal period. Although Bögner et al. [19] attribute release of NOx on switching from lean-rich as a slow reduction of noble metal sites and a rapid increase in NOx surface coverage, Fridell et al. [3] believe that during rich operation, reduction of metal sites is rapid and that it is barium nitrate decomposition which is rate limiting. To confirm that the release of NO_2 and NO under such conditions was not driven by the presence of a Pt surface which was able to reduce NO_2 to NO, a similar experiment was performed using a Pt-free Ba/Al_2O_3 sample. Results were almost identical in terms of the progressively diminishing peak size due to released NOx but with an increasing contribution from NO. The total amount of NOx released by the Pt-free sample was less, but this can be attributed to the reduced NOx storage capacity in the absence of Pt [7]. The appearance of NO in the presence of hydrogen rather than NO_2 alone at temperatures below which Ba/Al_2O_3 has significant activity for NO_2 decomposition [9] and independent of the presence or absence of Pt indicates that direct reduction by hydrogen of nitrate on the Ba/Al_2O_3 support is possible.

Scheme (C), where the need for reduced Pt sites is required, is also discounted as being a significance route to NOx release on the basis of experiments where the reductant gases were switched at 473 K (Figs. 11 and 12). Should the progressive decrease in the NO_2:NO ratios as a function of increasing temperature in the presence of reductant result [12] from the increasing efficiency of Pt to catalyze NO_2 reduction as the surface sites are depleted of adsorbed oxygen, then switching to CO, which as a reductant released essentially no NO below 473 K (Fig. 6), would be expected to generate a very different TPD profile from that where CO alone was employed as reductant. However, the shape of the NO profile above 473 K was almost identical whether CO (Fig. 6) or hydrogen (Fig. 12) had been exposed to the catalyst below 473 K. This provides further evidence that it is not the nature of the platinum surface which controls the extent of reduction of the released NOx.

If direct interaction between stored NOx and reductant initializes the release of NOx as NO_2 or NO, then the FTIR spectra recorded during the isothermal experiments during H_2 pulsing should reveal the source of the released gases. Heating till the isothermal temperature of 610 K in air gave a spectrum for $Pt/Ba/Al_2O_3$ where bands at 1580, 1560, 1420, and 1298 cm^{-1} dominated, unlike spectra recorded at the equivalent temperature for $Pt/Ba/Al_2O_3$ during the TPRS in hydrogen/air/N_2 where bands at 1557, 1460, 1421, and 1332 cm^{-1} were the most intense features (Fig. 2, h). After three pulses, there was a dramatic loss in intensity at 1580 and 1298 cm^{-1} and very little NO_2 was released after this point. These bands are due to bidentate nitrate adsorbed on alumina with their clear resolution under these conditions, compared with spectra recorded at 298 K (Fig. 2, a) a consequence of their greater thermal stability compared with other adsorbed nitrates [5,7]. When the same pulse experiment was performed for a Pt-free sample, the spectrum was dominated by features at 1750, 1586, and 1298 cm^{-1} (chelating bidentate nitrate on alumina), 1343 and 1236 cm^{-1} (bridged bidentate nitrite on alumina) and 1480 cm^{-1} (linear nitrite on alumina) present for alumina alone. Features due to adsorption on alumina were of greater relative importance than those on baria as a consequence of the poorer baria dispersion on Pt-free catalyst. Although a gradual loss in band intensity was observed as a function of the number of hydrogen pulses over the Ba/Al_2O_3, all the cited bands were still dominant after 1 h at 610 K. The conclusions are as follows:

(a) Of all the adsorbed NOx species, chelating bidentate nitrates on alumina (1580, 1298 cm^{-1}) are the most thermally stable in air at 610 K [3,7].
(b) These species are also thermally stable on Ba/Al_2O_3 at 610 K in H_2, but in the presence of Pt, they are slowly decomposed. If NOx desorption followed by reduction over Pt is the principle mechanism, then these species should decompose irrespective of the presence or absence of Pt.
(c) As the peaks due to NO_2 and NO are released simultaneously during hydrogen pulsing, giving a gradual increase in the $NO:NO_2$ ratio, then assuming that Pt reduction is rapid under these conditions [3], reduction of nitrate species on alumina might involve hydrogen activated over Pt and spillover.
(d) Reduction (release of NO) from NOx stored over the baria component does not require the presence of Pt, indicating that baria is capable of activating hydrogen.

Unlike the case of hydrogen, where NOx desorption was followed by simultaneous release of NO and NO_2 irrespective of whether operation was under isothermal or temperature-programed conditions, the use of CO as reductant generated first NO_2, followed by NO. Again, as NO release occurred below the temperature at which Ba/Al_2O_3 exhibits significant activity (773 K) for the decomposition reaction of NO_2 to yield NO and oxygen [9], the appearance of NO giving a maxima at ca. 553 K (Fig. 6) must invoke a role for the reductant. However, NO was released (Fig. 6) from around 423 K while significant CO conversion was observed only above 560 K, thereby eliminating any major role for mechanism B where nitrate was displaced due to formation of carbonate. Results could be interpreted in terms of a gradual change from scheme (1) $(NO_3{}^-)_2 \Leftrightarrow O^{2-} + \frac{1}{2}O_2 + 2NO_2$ to scheme (2) $(NO_3{}^-)_2 \Leftrightarrow O^{2-} + O_2 + NO_2 + NO$ between 298 and 560 K, although the transition could not have been driven by reduction in gas-phase oxygen consumption (mechanism A) as no measurable conversion of CO to CO_2 was detected (Fig. 7) within this temperature range. If the decomposition or reduction of NO_2 to NO was catalysed by Pt, then it is clear that this must have proceeded over an oxidized Pt surface as the FTIR spectra (Fig. 5A) clearly indicate that the adsorption sites available for CO [10] were oxidized (2120 cm^{-1}) rather than reduced (2080 cm^{-1}) at least until 500 K. Nova et al. [12] suggest that release of NO in the presence of reductant is the consequence of nonselective reduction over Pt–O species rather than desorption–decomposition of stored nitrite/nitrate species. However, to distinguish between NO formation as a result of NO_2 decomposition or reduction by CO is not easy on the basis of the mass spec plots as the contribution made by CO_2 produced by reaction with the maximum amount of stored NOx would not be readily detected on the scale employed in Fig. 8.

Experiments performed under identical conditions over a Pt-free catalyst failed to provide totally unambiguous insight into the role of the metal as the TPRS plots in the presence of CO showed release of both NO_2 and NO over the whole 298–873 K temperature range (Fig. 6) which may have been a consequence of the significant differences in Ba dispersion for Pt-containing and Pt-free samples. However, it is clear that NO may be formed by direct decomposition/desorption from the nitrite/nitrate in the absence of Pt [14]. However in support of a claim for a role of Pt–O in formation of NO rather than N_2 [14], Ba/Al_2O_3 released significant quantities of NO up to 873 K, whereas in the presence of Pt, very little NO was generated at temperatures (557 K) above which FTIR evidence (Fig. 5A, g) indicated the presence of reduced Pt sites. This would suggest that reduced Pt sites are required before complete reduction of stored NOx to N_2 is possible. Further evidence for this proposal was the appearance of bands due to NCO on the support (Fig. 5A, h and i) at temperatures for which Pt^0 sites were detected. The detection of this species is often used as an indication of the onset of N–O dissociation [20].

At the onset for the propene/O_2 reaction around 600 K as indicated by both mass spec (Fig. 10) and the gas-phase CO_2 signal in the FTIR spectra (Fig. 8A, g), only one resolved feature with maximum at 2120 cm^{-1} was detected indicative of CO (partial oxidation product) at oxidized Pt sites [10]. Although the band was quite broad and may have included lower frequency contributions due to CO on O-free sites, the oxidation of propene over an O-covered Pt site is consistent with our previous findings [7] and with Burch and Sullivan [21] who believe that propene from the gas-phase may react directly with an oxygen-covered Pt surface.

As for Pt/Al_2O_3 [10] reduced Pt sites were required for CO oxidation as indicated by the coincident temperatures for CO_2 detection (Fig. 7 and Fig. 5A, g) and the IR band due to CO adsorbed at Pt(0) sites (Fig. 5A, g). The light-off curve for CO oxidation was almost identical whether NOx was present or absent (Fig. 7), whereas light-off for H_2 (Fig. 4) and propene (Fig. 10) was significantly delayed when NOx was present. Although an ensemble requirement for C_3H_6 and H_2 adsorption but not for CO and related to higher surface oxygen coverage resulting from NO_2 exposure compared with molecular oxygen [22] would explain the relative light-off temperatures in the presence and absence of NOx, this is not consistent with all of the experimental data presented here, especially FTIR data of CO frequencies which indicate the extent of oxygen coverage at the point of light off. The H_2/O_2 reaction only proceeded during a temperature window where release of NOx was limited (Fig. 3) while the C_3H_6/O_2 reaction was delayed until 623 K by which point the majority of NOx had already been released (Fig. 9). These findings are consistent with an NOx(ad) inhibition of oxidation reactions as previously reported [7] and would be consistent with relatively uncompetitive (weak) adsorption of hydrogen and propene on Pt sites in the presence of NOx. The fact that the light off curves for CO were very similar in the presence and absence of NOx (Fig. 7) and that the onset of light off occurred at a temperature where maximum evolution of NOx took place indicates that CO/O_2 reaction was not inhibited by NOx. This implies that unlike hydrogen and propene CO was strongly adsorbed such that inhibition of the oxidation reaction was not observed.

5. Conclusions

NOx stored over a $Pt/Ba/Al_2O_3$ catalyst was released with a marked dependence on the nature of the gas composition. In the presence of air or nitrogen less than 10% of stored NOx was detected as NO whereas in the presence of reductant, both NO_2 and NO were detected in the gas phase, although the amounts depended on the reductant used. NO was released directly from the stored NOx rather than being a product of partial NO_2 reduction over the Pt, although the decomposition of certain forms of stored NOx was facilitated by the presence of Pt and may have involved spillover of activated reductant from Pt sites. Reduction of stored NOx to N_2 requires the presence of reduced Pt sites. High surface coverage, possibly by adsorbed NOx, led to delayed light-off for hydrogen and propene oxidation while CO oxidation reaction was unaffected.

Acknowledgment

We thank the Royal Society (London) for the award of a K.C. Wong fellowship (to Z.L.).

References

[1] N. Takahashi, H. Shinjoh, T. Iijima, T. Suzuki, K. Yamazaki, K. Yokota, H. Suzuki, N. Miyoshi, S. Matsumoto, T. Tanizawa, S. Tanaka, T. Tateishi, K. Kashara, Catal. Today 27 (1996) 63.
[2] S. Matsumoto, Catal. Surv. Jpn. 1 (1997) 111.
[3] E. Fridell, M. Skoglundh, B. Westerberg, S. Johansson, G. Smedler, J. Catal. 183 (1999) 196.
[4] J.M. Coronado, J.A. Anderson, J. Mol. Catal. 138 (1999) 83.
[5] Ch. Sedlmair, K. Seshan, A. Jentys, J.A. Lercher, J. Catal. 214 (2003) 308.
[6] J.A. Anderson, A.J. Paterson, M. Fernández-García, Stud. Surf. Sci. Catal. 130 (2000) 1331.
[7] J.A. Anderson, B. Bachiller-Baeza, M. Fernández-García, Phys. Chem. Chem. Phys. 5 (2003) 4418.
[8] J.A. Anderson, M. Fernández-García, J. Chem. Eng. A 78 (2000) 935.
[9] N.W. Cant, M.J. Patterson, Catal. Today 73 (2002) 271.
[10] J.A. Anderson, J. Chem. Soc., Faraday Trans. 88 (1992) 1197.
[11] J.A. Anderson, C. Marquez Alvarez, M.J. Lopez-Muñoz, I. Rodriguez Ramos, A. Guerrero Ruiz, Appl. Catal. B 14 (1997) 189.
[12] I. Nova, L. Castoldi, L. Lietti, E. Tronconi, P. Forzatti, Catal. Today 75 (2002) 431.
[13] F. Laurent, C.J. Pope, H. Mahzoul, L. Delfosse, P. Gilot, Chem. Eng. Sci. 58 (2003) 1793.
[14] N.W. Cant, M.J. Patterson, Catal. Lett. 85 (2003) 153.
[15] X. Li, M. Meng, P. Lin, Y. Fu, T. Hu, Y. Xie, J. Zhang, I. Chem. Eng. A 80 (2002) 190.
[16] A. Amberntsson, H. Persson, P. Engström, B. Kasemo, Appl. Catal. B 31 (2001) 27.
[17] J.A. Anderson, B. Bachiller-Baeza, M. Fernández-García, in: S.D. Jackson, J.S.J. Hargreaves, D. Lennon (Eds.), Catalysis in Application, RSC, London, 2003, pp. 296–301.
[18] L. Olsson, E. Fridell, M. Skoglundh, B. Anderson, Catal. Today 73 (2002) 263.
[19] W. Bögner, M. Krämer, B. Krutzsch, S. Pischinger, D. Voigtländer, G. Wenninger, F. Wirbeleit, M.S. Brogan, R.J. Brisley, D.E. Webster, Appl. Catal. B 7 (1995) 153.
[20] A. Martínez-Arias, M. Fernández-García, A. Iglesias-Juez, A.B. Hungría, J.A. Anderson, J.C. Conesa, J. Soria, Appl. Catal. B 31 (2001) 51.
[21] R. Burch, J.A. Sullivan, J. Catal. 182 (1999) 489.
[22] M.E. Bartram, R.G. Windham, B.E. Koel, Surf. Sci. 184 (1987) 57.